

Nematic phase with colossal magnetoresistance and orbital polarons in manganite $\text{La}_{1-x}\text{Sr}_x\text{MnO}_3$

M. Hennion,¹ S. Petit,¹ A. Ivanov,² D. Lamago,³ and J. P. Castellan^{3,1}

¹*Laboratoire Léon Brillouin, CEA, CNRS, Université Paris-Saclay, F-91191 Gif-sur-Yvette, France*

²*Institut Laue-Langevin, 71 Avenue des Martyrs, F-38000 Grenoble, France*

³*Institute of Solid State Physics, Karlsruhe Institute of Technology, D-76021 Karlsruhe Germany*

(Dated: April 30, 2019)

The origin of colossal magnetoresistance (CMR) is still controversial. The spin dynamics of $\text{La}_{1-x}\text{Sr}_x\text{MnO}_3$ is revisited along the Mn-O-Mn direction at $x \leq 0.5$, $T \leq T_C$ with a new study at $x=0.4$. A new lattice dynamics study is also reported at $x_0=0.2$, representative of the optimal doping for CMR. In large- q wavevector range, typical of the scale of polarons, spin dynamics exhibits a discrete spectrum, E_{mag}^n with n equal to the degeneracy of orbital-pseudospin transitions and energy values in coincidence with the phonon ones. It corresponds to the spin-orbital excitation spectrum of short life-time polarons, in which the orbital pseudospin degeneracy is lift by phonons. For $x \neq x_0$, its q -range reveals a $\ell \approx 1.7a$ size of polarons with a dimension $2d$ at $x = 1/8$ partly increasing to $\approx 3d$ at $x = 0.3$. At $x_0 = 0.2$ ($T < T_C$) two distinct q and energy ranges appear separated by $\Delta E(q_0 \approx 0.35) = 3\text{meV}$. The same $\Delta E(q_0)$ value separates two unusual transverse acoustic branches ($T > T_C$). Both characterize a nematic-phase defined by chains of "orbital polarons" of $2a$ size, distant from $3a$, typical of $x_0 = 1/6$. It could explain CMR.

PACS numbers:

The present work belongs to the rich research field of strongly correlated quantum materials^{1–7} which gives rise to high T_C supraconductivity and "colossal" magnetoresistance (CMR) properties. By doping ferromagnetic (F) cubic manganites, many anomalies appear in spin dynamics^{8–18} and lattice dynamics^{19–21} which are not reconciled up to now, so that, although the rôle of inhomogeneities was emphasized^{22–28}, no consensus exists to explain CMR. $\text{La}_{1-x}\text{Sr}_x\text{MnO}_3$, is considered as the the largest band compound²⁹. Here, CMR is maximum at $x_0 \approx 0.17$ and decreases beyond³⁰. One major interest of this compound, is that discrete energy features appear in spin dynamics, blurred in the narrow band $\text{La}_{1-x}\text{Ca}_x\text{MnO}_3$ ⁹. For insuring their meaning, we revisit the spin dynamics in a large doping range, namely at $x = 1/8$, $x_0 = 0.2$, representative here of the optimum doping for CMR, $x = 0.3$, and provide new measurements at $x = 0.4$. In addition, new transverse acoustic phonon excitations are reported at $x_0=0.2$ around T_C . A new analysis of spin dynamics is proposed, guided by the picture of "orbital polaron" introduced to describe the charge ordered (CO) states observed in narrow-band and pseudo-cubic compounds with x, y, z axes²⁹. It consists of one Mn^{4+} center, carrying the charge, with its first Mn^{3+} neighbors along x and y if the dimension is $2d$ consequence of the $2d$ F planes of the parent LaMnO_3 , or along x, y and z , at $x = 0.25$, with $3d$ dimension. Because of stericity, the polarons become $1d$ elongated along x and y , bound into zig-zag chains at $x = 0.5$ ²⁹. Whatever the dimension, the "size" of polarons is $2a$. In present study at $T \leq T_C$ and $T \geq T_C$ (T_C is the Curie temperature) spin and lattice dynamics obtained from inelastic neutron scattering may characterize orbital polarons with, at $x_0 \leq 0.2$, correlations which agree with a nematic or short-range charge-stripes structure².

The spin dynamics of Figure 1 exhibits mainly two distinct behaviors depending on the q -range, namely a Dq^2 law which occurs at the Curie temperature T_C in small- q range and a discrete spectrum, E_{mag}^n in large- q range. Such a description is typical of an inhomogeneous state. The Dq^2 law corresponds to the usual spin waves of a mean F state and the E_{mag}^n spectrum corresponds to the internal excitations of local inhomogeneities, either isolated, if q -independent, or correlated if q -dependent. The respective feed-back effects are also observed, indicated by discrete energy features in small- q range and by a specific q -dependent intensity in large- q one. In the picture of polarons of the CO states, the e_g orbital of Mn^{3+} ($3x^2 - r^2$ type) has a $p - d$ character and is elongated towards the Mn^{4+} center²⁹. This "pseudospin" is labelled T^α where $\alpha=x, y, z$ defines its orientation. In metallic state, due to the hopping or tunnelling of some charges, one expects short life-time polarons, with degenerated pseudospin orbital states. Their fingerprint appears in spin dynamics as follows. In Figure 1, the n number value increases from $n=4$ at $x = 1/8$ ($q = 0.5$) to $n \approx 6 - 7$ at $x_0 = 0.2$ and $x = 0.3$ and decreases to $n \approx 2 - 3$ at $x = 0.4$. This evolution agrees with that of the degeneracy of the orbital pseudospin states. Actually one expects $n = 4$ for the "in-plane" pseudospin states transitions as the charges are hopping within $2d$ space $((\alpha, \beta) = (x, y))$ gives rise to the (x, x) , (x, y) , (y, x) and (y, y) transitions), increasing to a larger value ($n \leq 9$) as charges are hopping in $3d$ space, until stericity reduces the degeneracy by approaching $x = 0.5$. Moreover, the E_{mag}^n energies exhibit a successive coincidence with the phonon ones reported for $x_0 = 0.2$ in Figure 3, but also measured for each sample, showing a specific evolution with x . At $x = 1/8$, due to the q -modulations of the spectrum, this successive coincidence concerns only $q = 0.5$

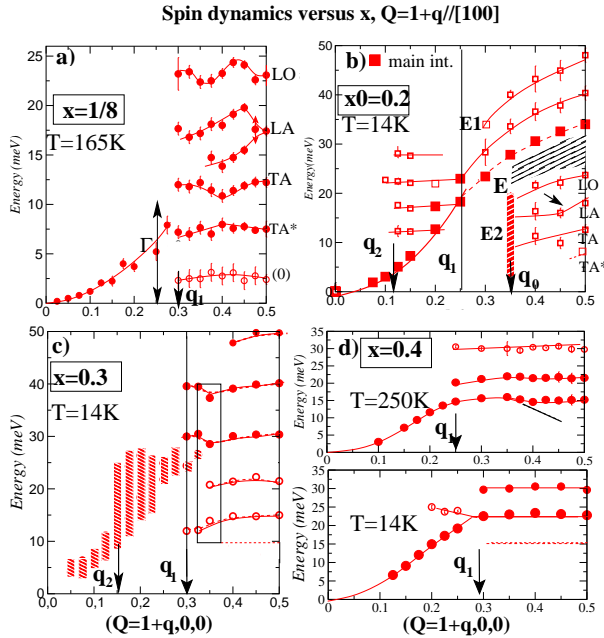


FIG. 1: Spin dynamics spectra of $\text{La}_{1-x}\text{Sr}_x\text{MnO}_3$ along Mn-O-Mn a) at $x=1/8$, $T=165\text{K}$. The empty circles have a distinct origin from that of the full ones (see the text). b) at $x_c=0.2$, $T=14\text{K}$. The hatched area indicates an anomalous energy separation between the $E1$ and $E2$ ranges. c) at $x=0.3$, $T=14\text{K}$. The rectangle outlines a softening anomaly at $q_0 = 0.35$. d) at nominal $x=0.4$ value, $T=14\text{K}$ (lower-level) and $T=250\text{K}$ (upper level) where a tendency for folding is shown by a dotted black line. For all x values, the continuous lines are guides for the eyes and the dashed ones ($x=0.2, 0.3, 0.4$) are badly defined energy levels due to the limited experimental resolution. The pattern style at $x=0.2$ and $x=0.3$ indicates unresolved excitations.

(zone boundary). At $x_0 = 0.2$ ($E < 25\text{meV}$), it concerns the q -dependent phonon energies and at $x = 0.3$ and $x = 0.4$, it concerns the phonon energies averaged on the q -range of E_{mag}^n . We have also checked that these excitations exhibit a magnetic and spin-flip character by using polarized neutrons under magnetic field (3.5 Teslas) at $x = 1/8$, $T = 140\text{K}$ ⁸. We conclude that the E_{mag}^n spectrum has a spin-orbital origin, in which the degeneracy of the pseudospin states transitions is lift by phonon energies. This is a dynamic Jahn-Teller effect. These low-energy excitations were actually predicted as orbital degeneracy occurs, with the disappearance of orbital ordering ($x \leq 0.1$) and of the corresponding high-energy "orbiton" excitations³¹. They are the consequence of the interplay between the spin S and orbital T degrees of freedom of Mn^{3+} ions^{31,32}. This "lift of degeneracy", is observed in the reciprocal space. The evolution of the energies with x is due to the decrease of the life-time τ of polarons, as the charge hopping frequency increases. At $x = 0.3$ and 0.4 (metallic state) the life-time τ of the polarons is shorter than the reverse frequency scale $1/f$ of the phonons. The degeneracy is lift by q -averaged phonon values on the $[0.3 - 0.5]$ q -range of single po-

larons. Using the relation $\ell = 0.5a/0.3$ ³³, this q -range defines a "dynamic size" $\ell \approx 1.7a$ in direct space, or a large contraction of the orbital polaron, compared to its $2a$ value in CO state. At $x = 1/8$ and $x_0 = 0.2$, the life-time is larger than $1/f$. The orbital degeneracy is lift by q -dependent energies connected through the lattice, determining the polaron's size and its correlations. At $x_0 = 0.2$, two sets of energy ranges appear separated by $\Delta E(q_0 \approx 0.35)$ (Figure 2-b), attributed to in-plane ($E < 25\text{meV}$) and out-of-plane ($E > 25\text{meV}$) pseudospin states transitions. Their q -characteristics agree with polarons of size $2a$ ³³, bound into chains distant from $3a$, along which spin waves propagate. Such correlations typical of the $x = 1/6 \approx 0.17$ doping value define a nematic phase with short life-time. This picture agrees with the observation of two unusual transverse acoustic phonon branches at $T \geq T_C$. $\Delta E(q_0 \approx 0.35) = 3\text{meV}$ defines a charge-orbital-lattice energy which stabilizes this phase.

The quasi-metallic regime: $x=1/8$. Figure 1-a shows the spin dynamics along Mn-O-Mn measured at $T = 165\text{K}$, in the quasi-metallic state above the charge-ordered state ($T \geq T_{\text{CO}} = 159\text{K}$) with $T \leq T_C = 181\text{K}$. Raw data are displayed in Supp-Mat. 1 and 2. The discontinuity in q -scale at $q_1 = 0.3$ is meaningless in energy scale, when considering the damping Γ of the excitations for $q < 0.3$. The E_{mag}^n spectrum consists of four energy values $E = 7.8, 12, 17$ and 22.2 meV at $q = 0.5$ which coincide successively with the $q=0.5$ values of the transverse and longitudinal acoustic and first optical phonon excitations of Figure 3-a. The empty circles, temperature dependent, could correspond to an anisotropy energy for Mn spins on the scale of polarons. The E_{mag}^n spectrum arises at T^* , with $250\text{K} < T^* < 292\text{K}$, well above T_C from a paramagnetic signal, in agreement with the value provided by NMR experiments³⁴. This can be seen in Supp. Mat. 1-b and 1-b'. E_{mag}^n corresponds to the spin-orbital excitation spectrum of polarons with $2d$ character⁸. The q -range $[0.3 - 0.5]$ determines a "dynamic size" $\ell \approx 1.7a$ ³³, or a lattice contraction with respect to the $2a$ value in CO state²⁹. The correlations will be analyzed elsewhere.

The 2d-3d cross-over regime with CMR: $x_0=0.2$, $T_C=301\text{K}$. **A- The spin dynamic spectrum** measured at $T = 14\text{K}$ and reported in Figure 1-b, exhibits a change in energy scale by a factor 2 with respect to that of $x = 1/8$. Raw data are reported in Supp-Mat. 1. In large q -range, at $q_0 = 0.35$, an anomalous interval $E = 8\text{meV}$ appears, larger by $\Delta E = 3\text{meV}$ than the interval $\approx 5\text{meV}$ of the lower energy range. It is indicated by the hatched area in Figure 2-b. It defines a $\Delta E(q_0 \approx 0.35) = 3\text{meV}$ gap energy which separates two sets of discrete spectrum, $E2 \leq 25\text{meV}$ (in-plane degenerated pseudospin states as for $x = 1/8$), and $E1 \geq 25\text{meV}$ (out-of-plane ones). $E2(q)$ appears at $q_0 \geq 0.35$, in coincidence with q -dependent phonon energies. The coincidence is specially well observed for $LA(q)$ (see the arrow at $q = 0.45$ in Figure 1 and 3). Within our exper-

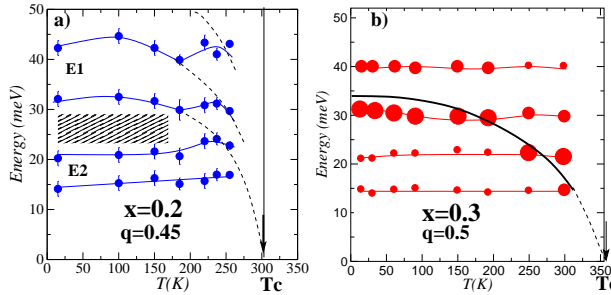


FIG. 2: Comparison between the temperature evolution of the four central energies of the E_{mag}^n spectrum **a**) at $x_c=0.2$ for $q = 0.45$ and **b**) at $x = 0.3$ for $q = 0.5$. The dashed and continuous lines are guides for the eyes. In (b) the relative variation of the intensity of the i energy values is shown by circles of varying size, providing the variation of the energy values (interpolated) with maximum of intensity (black line).

perimental accuracy, q_0 could be equal to $q_0 = 0.33 = 1/3$. Therefore, the excitations reveal propagating spin-orbital waves with a maximal $\lambda_0 = 2\pi/q_0 \approx 3a$ period for the Mn^{3+} spatial distribution along x or y . $E1(q)$ related to the z direction of one domain, may be analyzed in two components, a q -independent energy on the $[0.25 - 0.5]$ q -range, defining a $2a$ scale attributed to a phonon energy, and a q -dependent component in continuity with the Dq^2 law of the small- q range, attributed to spin waves. Such a superimposition, indicate that the spin waves should propagate specifically along the z direction as in an inhomogeneous F state. This agrees with the existence of chains of polarons. Actually, the discrete spectrum, observed by feedback, down to $q \approx 0.125$, defines a $\approx 4a$ value³³, as for two neighbor polarons or small chains on a straight line. Due to a sum rule of the magnetic intensity in favor of the $E = 0$, $q = 0$ limit of spin wave dispersion, no longer size, if any, can be experimentally observable. The period $2a$ along z with a distance $3a$ along x or y for $1d$ polarons, characteristic of the planar $x = 1/6 = 0.17$ doping value, corresponds to a nematic phase² with short lifetime. The existence of several branches in $E1$ and $E2$, results from the lift of degeneracy of the correlated orbital polarons which define one domain, by a dynamic Jahn-Teller effect. The degeneracy should arise from the fast motion of boundaries, or defects of periodicity, charged, responsible of the metallicity. The temperature dependence of $E1(T)$ and $E2(T)$ at $q = 0.45$, displayed in Figure 2-a confirms this analysis, at least up to $T = 200K$, since, beyond, the characteristics are blurred. $E1(T)$ consists of constant energy values (assumed to lie at phonon energies) on which is superimposed a temperature dependent component typical of the stiffness constant $D(T)$, corresponding to the spin-wave contribution. In contrast, $E2(T)$ is temperature independent (phonon energies only). One may expect that a magnetic field applied at T_C should induce the growing of domains with chains aligned with the field. Since the chains are also considered as paths for mobile charges²,

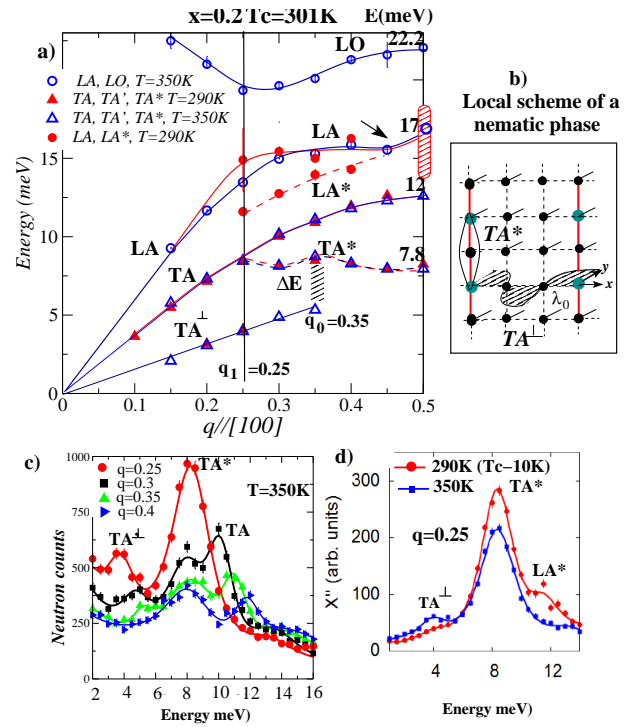


FIG. 3: **a)** Lattice dynamic spectrum ($E \leq 25$ meV) for $T = 350K$ (full symbols) and $T = 290K$ (empty symbols) measured at $x_0=0.2$. The measurements were performed on the 1T spectrometer of the Orphee reactor. The pattern style at $E=15$ meV indicates unresolved excitations at $T=290K$. The error bar is within the symbol's size. **b)** Local scheme of a nematic phase, with Mn^{3+} (black circles) and Mn^{4+} ions (cyan circles). **c)** Raw data of acoustic excitations as a function of q for $T \geq T_C$ and in **d**) at $q = 0.25$, $T \geq T_C$ and $T \leq T_C$, corrected from the Bose factor. There, the scattering of magnetic origin is a background with intensity weighted by the form factor of Mn.

these charge correlations should explain the CMR property. The anomalous spin dynamics along [111] agrees with that observed along [100] (Sup. Mat. 3).

B - Two unusual transverse acoustic branches were measured at $T = 350K$ ($T > T_C$) and $T = 290K$ ($T < T_c$) along Mn-O-Mn, displayed in Figure 3-(a) with the usual ones, of longitudinal and transverse character ($E \leq 25$ meV) previously reported¹⁹. At $T = 350K$, a nearly constant-energy value, $E \approx 8$ meV, is observed in the $[0.25 - 0.5]$ q -range, labeled TA^* , connected with the $TA(q)$ branch of the usual $3d$ pseudo-cubic structure at $q_1=0.25$. At lower energies, a $TA^\perp(q)$ branch is observed, up to $q_0 \approx 0.35$, where a small shift in energy appears in TA^* , defining a $\Delta E(q_0 \approx 0.35) \approx 3$ meV energy separation. At $T = 290K$, the $TA^\perp(q)$ branch progressively disappears as the metallic character increases, whereas the TA^* one persists with the same energy anomaly at $q_0 \approx 0.35$. Concomitantly new excitations occur in the $[0.25 - 0.5]$ q range, such as LA^* just below the usual $LA(q)$ branch. Finally, the intensity of $TA^*(q = 0.25)$, increases below T_C , in contradiction with the Bose factor,

reminding observations at higher energy^{14,20}. Raw data are displayed in Figure 3 (c, d), with intensity corrected from thermal Bose factor. We have checked that the TA^* branch does not exist along the [110] symmetry direction. The observation of two unusual transverse acoustic excitations agrees with the existence of two distinct q^x and q^z wavevectors in the pseudo-cubic structure. The TA^* branch is attributed to excitations transverse to q^z . They are stationary, defined on the $[0.25 - 0.5]$ q scale, corresponding to a size $2a$ (Figure 3-b). This value, characteristic of ordered polarons, supports the existence of chains along z . Due to their transverse character, their energy is unsensitive to the binding along z , so that it is equal to that, $TA(q = 0.25) = 8$ meV, of the pseudo-cubic structure. At lower energy, for $q \leq 0.35$ or $\lambda \geq 3a$, the $TA^\perp(q)$ branch indicates excitations transverse to the perpendicular q^x wave-vector. It reveals the existence of a weaker and long-range coupling, defining a maximal $q_0 \approx 0.35$ value or a minimal $\lambda = 3a$ periodic distance. It reminds the weak coupling due to the intrinsic strain field, related to the finite-size domain, observed in CO states³⁷. This coupling could become much stronger as the domain-size becomes that of clusters. This corresponds to a nematic phase picture². The cut-off $q_0 \approx 0.35$ common to the $q \geq 0.35$ excitations observed in spin dynamics, defines a $\Delta E(q = 0.35) = 3$ meV energy. It characterizes the stability of this nematic-phase, resulting from short-range (orbital) and long-range (lattice) couplings. The $2d$ spatial extension of the cluster is undetermined here. q^y is irrelevant. At $T \leq T_C$, the increase of intensity of $TA(q = 0.25)$, alike a "dynamic Bragg peak", indicates a phase-coherence along z as charged defects become mobile, or a period $2a$ for the TA^* excitations like for chains of polarons. The $TA^\perp(q)$ branch disappears as the lifetime of polarons which decreases with the motion of the boundaries becomes shorter than $1/f$ defined by $E \leq 5$ meV, whereas the TA^* branch, at $E = 8$ meV, persists.

The metallic regime. At $x = 0.3$ ($T_C = 358$ K), the E_{mag}^n spectrum reported in Figure 1-c with raw data in Supp-mat-1-f-g is nearly q -independent with $q_1 \approx 0.3$. The energy values $E = 15$ meV and $E = 21$ meV of the E_{mag}^n spectrum ($E < 25$ meV), slightly smaller than those observed at $x = 1/8$, agree with q -averaged phonon ener-

gies on the $[q_1 - 0.5]$ range of the polarons. Here, the n number could be limited by the experimental energy window. An anomalous softening is observed at $q_0 = 0.35$, outlined by the rectangle in Figure 1-c. It suggests the proximity of a structure typical of $x = 1/3$, which is the optimal value for CMR in $\text{La}_{1-x}\text{Ca}_x\text{MnO}_3$. The distribution of energy with maximum of intensity in the E_{mag}^n defines a $E(I_{\text{max}})(q, T)$ function reported in Figure 2-b (black line), which decreases as $D(T)$ by approaching T_C . This evolution, feed-back of the small- q excitations on the large- q ones, strongly differs from that observed at $x_0 = 0.2$. In small q -range, an unresolved discrete spectrum is observed down to $q = 0.15$, as at $x_0 = 0.2$. **At nominal $x = 0.4$ value** ($T_C = 315$ K corresponds to $x \approx 0.5$ ³⁵) the E_{mag}^n spectrum displayed in lower Figure 1-d with raw data in Supp-Mat 1-h, exhibits the same energy values as for $x = 0.3$. The main change is a strong decrease of the n value (≈ 2 at $T = 14$ K). There, the T_C and D values ($T = 14$ K), are smaller than those observed at $x = 0.3$ ³⁶. The origin of such a decrease appears at $T = 250$ K in upper Figure 1-d where q_1 is shifted to $q_1 \approx 0.25$, whereas the whole spectrum exhibits a tendency for folding, outlined by the dotted black line. This reveals the proximity of a charge ordered state, hindered by the occurrence of the F metallic state at T_C .

In conclusion, the present analysis of the large- q range of spin dynamics in terms of spin-orbital excitations³¹ provides a microscopic and quantitative description of charge-induced inhomogeneities or polarons, determining their size, dimension d , and correlations. At optimal doping for CMR, spin and lattice dynamics reveal charge-correlations typical of a nematic-phase with $x = 1/6$ (≈ 0.17). A similar phase has been suggested in $\text{La}_{1-x}\text{Ca}_x\text{MnO}_3$, at equivalent $x_0(\text{Ca}) \approx 1/3$ doping by TEM experiment³⁷, so that a common process appears for CMR in both cases at two distinct x_0 values. This state is analogous to the smectic one, long-range, observed in several antiferromagnetic (AF) compounds whatever the Mn, Cu or Ni magnetic atoms^{5-7,37}. The newest result is its observation in a metallic state.

Acknowledgements The authors are very indebted to S. Aubry, Y. Sidis, F. Moussa, B. Hennion and F. Onufrieva for enlightning discussions.

¹ Tranquada J., Sternlieb B. J., Axe D., Nakamura Y. and Ushida S., *Nature* **375**, 561-563 (1995)

² Kivelson S. A., Fradkin E. and Emery V. J., *Nature* **393**, 550 (1998)

³ Dagotto E., *Science* **309**, 257-62 (2005)

⁴ Ulrich H. and Braden M. *Physica C*, 481,31 (2012)

⁵ Anissimova S., Parshall D., Lamago D., Gu G. D., Lumsden M. D., Chi Songxue, Fernandez-Baca J. A., Albernathy D. L., Tranquada J. and Reznik D., *Nat. Commun.* **5** 3467 (2014)

⁶ Tao J., Sun K., Yin W. -K, Xin H., Wen J. G., Luo W., Pennycock S. J., Tranquada J. M. Zhu Y. et al., *Sc. Report*

6, 37624 (2016)

⁷ Liu Mengkun, Sterbach Aaron J., Basov D. N. *Prog. Phys.* **80** 014501 (2017)

⁸ Hennion M., Moussa F., Lehouiller P., Reutler P., Revcolevschi A., *Phys. Rev. B* **73**, 104453 (2006)

⁹ Petit S., Hennion M., Moussa F., Lamago D., Ivanov A., Mukhovski Y. M., Shulyatev D., *Phys. Rev. Lett.* **102**, 207201 (2009)

¹⁰ Moussa F., Hennion M., Wang F., Kober P., Rodriguez-Carvajal J., Reutler P., Pinsard L., Revcolevschi A., *Phys. Rev. B* **67** 214430 (2003)

¹¹ Lynn J., Erwin R. W., Borchers J. A., Huang Q., Santoro

A., Peng J. L., Li Z. Y., Phys. Rev. Lett. **76** 4046 (1996)

¹² Vasiliu-Doloc L., Lynn J. W., Moudden A. H., de Leon-Guevara A. M., Revcolevschi A. Phys. Rev. B **58**, 14913 (1998)

¹³ Dai Pengcheng, Hwang H. Y., Zhang Jiandi, Fernandez-Baca J. A., Cheong S. W., Kloc C., Tomioka Y., Tokura Y., Phys. Rev. B **61** 9553 (2000)

¹⁴ Zhang J., Dai P., Fernandez-Baca J. A., Plummer E. W., Tomioka Y., Tokura Y., Phys. Rev. Lett **86**, 3823 (2001)

¹⁵ Fernandez-Baca J. A., Dai P., Kawano-Furukawa H., Yoshizawa H., Plummer E. W., Katano S., Tomioka Y., Tokura Y., Phys. Rev. B **66**, 054434 (2002)

¹⁶ Endoh H., Hirakawa H., Tomioka Y., Tokura Y., Nagaosa N., Fujiwara T., Phys. Rev. Lett. **94** 017206 (2005)

¹⁷ Ye F., Dai P., Sha H., Fernandez-Baca J. A., Lynn J. W., H. Kawano-Furukawa, Tomioka Y., Tokura Y., Zhang J., Phys. Rev. Lett. **96**, 047204 (2006)

¹⁸ Viret M., Glattli H., Fermon C., de Leon-Guevara A. M., Revcolevski A., Europhys. Lett. **42** 301-306 (1998)

¹⁹ Reichardt W. and Braden M., Physica B **263-264** , 41 (1999)

²⁰ Weber F., Argyriou D.N., Prokhnenco O., Reznik D., Phys. Rev. B **88**, 241106(R) (2013)

²¹ Maschek M., Lamago D., Castellan J. P., Bozak A., Reznik D., Weber F., Phys. Rev. B **96** 045112 (2016)

²² Millis A. J., Mueller R., Shraiman B. I., Phys. Rev. B **54** 5405 (1996)

²³ Varma C. Phys. Rev. B **54**, 7328 (1996)

²⁴ Killian R. and Khaliulin G., Phys. Rev. B **58**, 11841 (1998)

²⁵ Moreo A., Mayr M., Feiguin A., Yunoki S., Dagotto E., Phys. Rev. Lett. **84**, 5568 (2000)

²⁶ Alexandrov S., Devreese J. T., "Advances in polarons" Springer Science, Business Media (2009)

²⁷ Hartinger Ch., Mayr F., Loidl A., Kopp T., Phys. Rev. B **73**, 024408 (2006)

²⁸ Cengiz S., Alvarez G., Dagotto E., Phys. Rev. Lett. **105**, 097203 (2010)

²⁹ Mizokawa T., Khomskii D. I., Sawatzky G. A., Phys. Rev. B **61**, R3776 (2000) and **63**, 024404 (2000)

³⁰ Urushibara A., Moritomo Y., Arima T., Asamitsu A., Kido G., Tokura Y. , Phys. Rev. B **51**, 14101 (1995)

³¹ Van den Brink J., Stekelenburg W., Khomskii D. I., Sawatzky G. A., Kugel K. I., Phys. Rev. B 58, 10276 (1998)

³² Kugel K. I. and Khomskii D. I., Sov. Phys. Usp. **25**, 231 (1982)

³³ From the q-range (q-independent) of local excitations defined by acoustic lattice energies, such as the spin-orbital excitations, for which no dynamical structure factor is expected, a "dynamic size" can be obtained by the relation $\ell = 0.5a/q_1$ as follows. Consider first a local interaction between two neighbor sites distant from a in a periodic lattice. It should give rise to an energy lying at the $q = 0.5$ value (zone boundary) of the reciprocal space. If the interaction spreads between two atomic sites distant from $\ell = 2a$ (or $\ell = 4a$,..) the excitation energy will be observed at the zone boundary of the corresponding virtual reciprocal space, $q_1=0.25$, (or $q_2=0.125$, etc), up to the $q=0.5$ value of the real reciprocal space. It should spread in the $[0.25 - 0.5]$, ($[0.125 - 0.5]$ etc.) q-ranges, yielding the $\ell = a/2q_{1,2}$ relation. The case of q_1 slightly distinct from 0.25, indicates a local dynamic discommensuration.

³⁴ Deisenhofer J., Braak D., Kruggvon Nidda H.-A., Humberger J., Eremina R. M., Ivanshin V. A., Bambashov A. M., Jug G., Loidl A., Kimura T., and Tokura Y., Phys. Rev. Lett. **95** 257202 (2005)

³⁵ Hemberger J., Krimmel A., Kurz T., Krug von Nidda H. A., Ivanov V. Yu, Mukhin A. A., Balbashov A. M., Loidl A. , Phys. Rev. B **66**, 094410 (2002)

³⁶ Moussa F., Hennion M., Kober-Lehouelleur P., Reznik D., Petit S., Moudden H., Ivanov A., Mukovskii Ya. M., Privezentsev R., Albenque-Rullier F., Phys. Rev. B **76**, 064403 (2007)

³⁷ Tao J. and Zuo M., Phys. Rev. B **69**, 180404R (2004)

³⁸ Van den Brink J., Physica B **312-313**, 743 (2002)